Frontal cortical regions associated with attention connect more strongly to central than peripheral V1

Sara A. Sims[a,*], **Pinar Demirayak**[b], **Simone Cedotal**[b], **Kristina M. Visscher**[b]

[a]Department of Psychology, University of Alabama at Birmingham, United States

[b]Department of Neurobiology, University of Alabama at Birmingham, United States

Abstract

The functionality of central vision is different from peripheral vision. Central vision is used for fixation and has higher acuity, making it useful for everyday activities such as reading and object identification. The central and peripheral representations in primary visual cortex (V1) also differ in how higher-order processing areas modulate their responses. For example, attention and expectation are top-down processes (i.e., high-order cognitive functions) that influence visual information processing during behavioral tasks. This top-down control is different for central vs. peripheral vision. Since functional networks can influence visual information processing in different ways, networks (such as the Fronto-Parietal (FPN), Default Mode (DMN), and Cingulo-Opercular (CON)) likely differ in how they connect to representations of the visual field across V1. Prior work indicated the central representing portion of V1 was more functionally connected to regions belonging to the FPN, and the far-peripheral representing portion of V1 was more functionally connected to regions belonging to the DMN.

Our goals were (1) Assess the reproducibility and generalizability of retinotopic effects on functional connections between V1 and functional networks. (2) Extend this work to understand structural connections of central vs. peripheral representations in V1. (3) Examine the overlapping eccentricity differences in functional and structural connections of V1. (4) Examine the major white matter tracks connecting central V1 to frontal regions.

We used resting-state BOLD fMRI and DWI to examine whether portions of V1 that represent different visual eccentricities differ in their functional and structural connectivity to functional networks. All data were acquired and minimally preprocessed by the Human Connectome Project. We identified central and far-peripheral representing regions from a retinotopic template.

*Corresponding author. snolin@uab.edu (S.A. Sims).

Functional connectivity was measured by correlated activity between V1 and functional networks, and structural connectivity was measured by probabilistic tractography and converted to track probability. In both modalities, differences between V1 eccentricity segment connections were compared by paired, two-tailed *t*-test. A spatial permutation approach was used to determine the statistical significance of the spatial overlap between modalities. The identified spatial overlap was then used in a deterministic tractography approach to identify the white matter pathways connecting the overlap to central V1.

We found (1) Centrally representing portions of V1 are more strongly functionally connected to frontal regions than are peripherally representing portions of V1, (2) Structural connections also show stronger connections between central V1 and frontal regions, (3) Patterns of structural and functional connections overlaps in the lateral frontal cortex, (4) This lateral frontal overlap is connected to central V1 via the IFOF.

In summary, the work's main contribution is a greater understanding of higher-order functional networks' connectivity to V1. There are stronger structural connections to central representations in V1, particularly for lateral frontal regions, implying that the functional relationship between central V1 and frontal regions is built upon direct, long-distance connections via the IFOF. Overlapping structural and functional connections reflect differences in V1 eccentricities, with central V1 preferentially connected to attention-associated regions. Understanding how V1 is functionally and structurally connected to higher-order brain areas contributes to our understanding of how the human brain processes visual information and forms a baseline for understanding any modifications in processing that might occur with training or experience.

Keywords

V1; Structural connectivity; Functional connectivity; Visual eccentricity; Functional networks

1. Introduction

The function of central vision is different from peripheral vision. Central vision is used for fixation and has higher acuity, making it useful for reading and object identification (Larson and Loschky, 2009; Pelli et al., 2007; Trouilloud et al., 2020; Yoo and Chong, 2012). Peripheral vision has lower acuity but is essential for visual tasks such as visual search and getting the gist of a scene (Larson and Loschky, 2009; Rosenholtz, 2016; Trouilloud et al., 2020). Differences in acuity between peripheral and central vision alone do not provide a full explanation of the extent of disparity in visual ability (Levi et al., 1985; Levi et al., 1984). Information processing of central and peripheral visual information also differs. Peripheral visual information is processed faster than central information (Lu et al., 2002), and this fast processing helps determine objects' salience within the visual field. This enables the visual system to direct saccades, fast eye movements, to a salient location (Lu et al., 2002). When central vision orients to the salient location, it provides high acuity information and distinguishes it from competing, distracting information (Lu et al., 2002).

The human primary visual cortex (V1) is organized along the calcarine sulcus in a progression of posterior representations of central vision (central V1) to anterior

representations of peripheral vision (far-peripheral V1) (Duncan et al., 2007; Engel et al., 1997; Fox et al., 1987). The anatomical regions representing central and peripheral V1 differ in their cortical thickness (Burge et al., 2016). The central representing portion of V1– the part of the visual field used for fixation – has a thicker cortex compared to the peripheral representing cortex in individuals with healthy vision (Burge et al., 2016).

There has been extensive prior research into the physiological differences between central and peripheral V1. Encoding of visual information differs within V1 representations of central and peripheral visual fields. The area of V1 devoted to central vision is much larger than that devoted to processing information from the peripheral visual field (Azzopardi and Cowey, 1993; Horton and Hoyt, 1991). In other words, the cortical magnification factor (square-mm of cortex devoted to each square-degree of visual angle) is greater for central vision than peripheral vision. Receptive field size is greater for neurons in peripheral V1 than in central V1 (Hubel and Wiesel, 1974). As eccentricity (distance from the center) increases, cortical magnification decreases, and receptive field size increases across human V1 and nearby visual areas (Harvey and Dumoulin, 2011).

Central and peripheral V1 also differ in how higher-order processing areas modulate their responses. Functional properties of cortical neurons are adaptive; top-down demands of high-order cognitive processing tasks influence their response (Gilbert and Li, 2013). For example, attention and expectation are top-down processes (i.e., high-order cognitive functions) that influence visual information processing during behavioral tasks (Gandhi et al., 1999; Somers et al., 1999; Tootell et al., 1998; Yeshurun and Carrasco, 1998). This top-down control is different for central vs. peripheral vision. Attention influences the spatial summation of receptive fields so that spatial summation in foveal cells decreases and spatial summation in the peripheral cells in V1 increases (Roberts et al., 2007). Psychophysiological data demonstrates that top-down influences on central vision stimuli are more potent than peripheral vision stimuli (Chen and Treisman, 2008; Zhaoping, 2017). Similarly, attentional suppression of distractors is greater for central vision than peripheral vision (Chen and Treisman, 2008). Vision representations are known to interact strongly with higher-order brain networks (eg. (Casarsa De Azevedo, 2019; Furl, 2015; Gazzaley et al., 2007; Griffis et al., 2015; Mantini et al., 2009; McMains and Kastner, 2011; Yeshurun and Carrasco, 1998), and these interactions appear to be distinct for central and peripheral vision.

Resting-state functional networks are groups of brain regions whose activity is temporally correlated at rest (Zalesky et al., 2014). One way to identify a functional network is through clusters of correlated activity in the cortex (Yeo et al., 2011). The fronto-parietal network (FPN) is important for directing attentional control (Zanto and Gazzaley, 2013), the cingulo-opercular network (CON) is involved in the maintenance of task demands (Coste and Kleinschmidt, 2016), and the default mode network (DMN) is less active when there are attentional or task goals (Raichle, 2015) and instead is thought to support tasks such as memory retrieval and semantic processing (Binder, 2012; Gerlach et al., 2011; Sestieri et al., 2010; Spreng, 2012). Since functional networks can influence visual information processing in different ways, networks likely differ in how they connect to representations of the visual field across V1. There are also feedforward connections between V1 and functional

network regions, as evidenced by the fact that strong stimulus-driven signals are observed in higher-order brain regions (Katsuki and Constantinidis, 2014).

Previous work in our lab has investigated how the central-to-peripheral cortical organization of V1 influences functional connectivity between V1 and the rest of the cortex (Griffis et al., 2017). This prior work showed retinotopic patterns of functional connectivity between V1 and functional networks during resting fixation. Specifically, the central representing portion of V1 was more functionally connected to regions belonging to the FPN, and the far-peripheral representing portion of V1 was more functionally connected to regions belonging to the DMN. The fact that, as described above, central vision is under different top-down control than peripheral vision might underlie its preferential connection to the FPN, which is related to directing attentional control and has been shown to facilitate bottom-up and top-down attentional processes for visual information (Katsuki and Constantinidis, 2014). The role of far-peripheral vision in environmental monitoring and the need to suppress visual information from this portion of the visual field during central fixation might be the reason for preferential connectivity to the task-negative DMN (Li, 2002). However, this previous work was limited by small sample size (i.e., 20 participants) and design (i.e., data were acquired during the resting fixation blocks of a visual task) issues (Griffis et al., 2017). These limitations leave questions regarding whether previous functional findings extend to free viewing during rest in a larger sample and, critically, how these effects relate to differences in the anatomical (i.e., white matter) connections of central vs. peripheral V1. The observed functional connections could arise from direct connections between two areas or and alternatively from weighted multi-synaptic connections (Honey et al., 2009; Vázquez-Rodríguez et al., 2019).

While brain anatomy is relatively fixed in adulthood, a healthy brain adapts with changes in structural connections with experience and age (Davis et al., 2009). White matter tracts correspond to direct connections between brain regions (Jbabdi and Johansen-Berg, 2011; Maier-Hein et al., 2017; Takemura et al., 2017). Structural connections can be studied in-vivo in humans with diffusion-weighted MRI and tractography. Major white matter tracts that connect to the occipital lobe, such as the inferior fronto-occipital fasciculus (connects occipital lobe to the lateral prefrontal cortex) and the inferior longitudinal fasciculus (connects occipital lobe to anterior temporal lobe), have been well documented using tractography methods in humans (Takemura et al., 2017; Wu et al., 2016).

Traditional tracer studies that examine anatomical connections with retrograde and anterograde tracers have primarily been focused on visual areas and have not been expanded to investigate connectivity between visual areas and higher-order processing areas (Andersen et al., 1990; Lysakowski et al., 1988; Neal et al., 1990). Extensive work by Markov and colleagues indicated some evidence of connection from V1 to regions of the frontal and parietal cortex, including F5 (a frontal area involved in motor planning), 8l (frontal eye fields), and 7A (a parietal area involved in attention modulation and planning) and connection to V1 from area 8l (frontal eye fields) (Markov et al., 2014). However, the inferior fronto-occipital fasciculus has not been found in the macaque brain, which may explain why tracer studies investigating V1 have not helped inform human occipital-prefrontal cortex connections (Takemura et al., 2017).

The current study's goals are (1) to assess the reproducibility and generalizability of retinotopic effects on functional connections between V1 and functional networks found in prior work (Griffis et al., 2017). We aim to extend these findings in a new dataset collected under different task conditions (previous work used blocks of rest during a task with central fixation, and the current data was collected as part of a resting-state only scan). (2) Extend prior work on the retinotopic connectivity difference to structural connections between V1 and functional networks. (3) Examine regions of overlap between functional and structural connections. Since functional connectivity between two brain regions could reflect measurable structural connections, we used DWI to examine connections between regions (Adachi et al., 2012; Honey et al., 2009).

To address these goals, we used resting-state BOLD fMRI and DWI to examine if portions of V1 that represent different visual eccentricities differ in their functional and structural connectivity to functional networks. We found (1) substantial evidence that centrally representing portions of V1 are more strongly functionally connected to lateral frontal regions than are peripherally representing portions of V1, (2) Structural connections show the same pattern, with stronger connections between central V1 and frontal regions, in particular a lateral frontal portion of the FPN, and (3) the pattern of structural and functional connections is similar, suggesting that this lateral frontal functional connection pattern arises from a direct (uni-synaptic) structural connection. These results, coupled with relationships to prior work described in the discussion, are suggestive that the processing of central vision is mediated in part through direct connections to the lateral frontal cortex.

2. Methods

2.1. Participants

The study used diffusion-weighted imaging, resting-state functional imaging, and structural imaging data from the 900-subject release of the Human Connectome Project (HCP) dataset (Fig. 1). Participants in this dataset were healthy young adults between 22and 36 years of age who had normal or corrected-to-normal vision. Most subjects had at least one relative in the group; many of them are twins. Our hypotheses are not about individual differences, and due to the large sample size of the data, there is still a great deal of diversity in the sample; therefore, we did not treat related and unrelated samples separately. Using this relatively large sample size facilitates replication and extension of findings.

We excluded participants with structural abnormalities (e.g., tumors and extensive area brain damage) identified through HCP quality control. We then visually inspected the remaining data for white matter abnormalities. We excluded participants if their structural scans displayed large or punctate white matter hyperintensities easily detected by eye. In total, we excluded 114 subjects from the original 900 subject dataset. Seven hundred eighty-six healthy subjects passed quality control standards, including 335 males and 449 females (Fig. 1; see participant IDs in code repository). We excluded the fMRI data from four of them due to quality standards for functional comparison. Otherwise, we used the same participants in both structural and functional connectivity analyses.

2.2.   Data acquired by the human connectome project

All data were acquired and minimally preprocessed by the Human Connectome Project (Glasser et al., 2016; Sotiropoulos et al., 2013; Van Essen et al., 2013, 2012). Informed consent was obtained by the Human Connectome Project (Van Essen et al., 2013). The IRB for the University of Alabama at Birmingham reviewed our use of the HCP dataset and determined it exempt.

T1-weighted structural MRI, resting state fMRI and multi-shell diffusion weighted (DWI) MRI data were acquired using a customized Siemens 3T "Connectome Skyra" (Sotiropoulos et al., 2013). High-resolution three-dimensional MPRAGE, T1-weighted anatomical images (TR = 2400 ms, TE = 2.14 ms, flip angle = 8, FOV = 320×320 mm^2 , voxel size $0.7 \times 0.7 \times 0.7$ mm^3 , number of slices = 256, acceleration factor (GRAPPA) = 2) were used.

Functional magnetic resonance imaging (fMRI) data were acquired with a multi-band gradient-echo (GE) EPI sequence (voxel size = $2 \times 2 \times 2$ mm^3 ; TR= 720 ms; TE = 33.1 ms; flip angle = 52°; FOV = 208×180 mm^2 ; number of slices = 72) in four runs (each of them took approximately 15 min) with eyes open and related fixation on a cross on a dark background. Phase encoding direction was right-to-left for half of the scans and left-to-right for the other half of the resting-state scans.

For DWI, multi-band diffusion-weighted echo-planar (EP) images (voxel size = $1.25 \times 1.25 \times 1.25$ mm^3 ; TR= 5520 ms; TE = 89.5 ms; flip angle = 78°; MB = 3; FOV = 210×180 mm^2 ; number of slices = 111; b = 1000, 2000 and 3000 s/mm^2 , diffusion directions = 95, 96 and 97) were used. DWI data includes six runs (each of them took approximately 9 min and 50 s). Each gradient table was acquired with right-to-left and left-to-right phase encoding polarities which were then merged after distortion correction as part of the HCP Preprocessing Pipeline (Glasser et al., 2013).

2.3.   V1 eccentricity segment definitions

V1 eccentricity segments were hand-drawn within the Freesurfer fsaverage V1 label as described in a previous publication from our lab (Burge et al., 2016; Griffis et al., 2015, 2017). Previous work has shown that cortical anatomy is a reliable predictor of the retinotopic organization of V1 (Benson et al., 2012; Hinds et al., 2009; Hinds et al., 2008) so that the more posterior parts of the visual cortex represent more central portions of the visual field. The average eccentricity of each segment was estimated from Benson and colleagues' retinotopy template (Benson et al., 2014; Benson and Winawer, 2018). Based on this template, we identified three retinotopic regions: central vision (mean eccentricity estimates of 0–2.2° visual angle), mid-peripheral vision (mean eccentricity estimates of 4.1–7.3° visual angle), and far-peripheral vision (mean eccentricity estimates of 14.1–25.5° visual angle) (Fig. 2).

These V1 eccentricity segment ROIs were defined on FreeSurfer's fsaverage brain using the retinotopic template's eccentricity, and then we interpolated them to the individual subjects' cortical surfaces using FreeSurfer's anatomical registration.

2.4.   Functional network ROI definitions

We transformed the FPN, CON, and DMN labels created by (Yeo et al., 2011) from the Freesurfer fsaverage brain to individual anatomical space (Yeo et al., 2011). We used voxels within the gray matter corresponding to the network-ROIs as seed voxels for the functional connectivity analysis. We used voxels within the white matter corresponding to the network-ROIs as track seeds for the probabilistic tractography analysis. Voxels were identified using the Freesurfer mri_aparc2aseg command and then transformed into individual diffusion space.

2.5.   Data analysis

2.5.1.   Resting-State scan image preprocessing—The HCP minimal preprocessing pipeline that includes artifact removal, motion correction, and registration to common space was used (Fischl, 2012; Glasser et al., 2013; Jenkinson et al., 2012; Jenkinson et al., 2002; Van Essen et al., 2012). Along with the preprocessing steps already described by Glasser et al. (2013), we applied additional preprocessing steps on the residual BOLD data to reduce spurious variance not associated with the neural activity as described in this paragraph. We then censored the functional images for movement according to validated techniques (Carp, 2013; Griffis et al., 2017; Power et al., 2012). We replaced time points in which a participant moved more than 0.5 mm in one TR with an interpolated image from adjacent images. We excluded runs if the mean framewise displacement across the run was greater than 3 mm in any direction. We applied temporal band-pass filtering between 0.009 and 0.08 Hz. We applied regressors to reduce artifactual noise, including white matter and CSF signals and motion parameters that we extracted during motion correction for each subject from the previous step. Surface reconstruction, the region of interest (ROI) label generation, and image registration were also visually inspected for all subjects to ensure the automated computations' accuracy. Next, we concatenated both the acquisitions (those collected right-to-left and those collected left-to-right) into a single 4D volume for the functional connectivity analysis.

2.5.2.   Functional connectivity analysis—Functional connectivity refers to synchronization between time courses of activation between two brain areas due to the similar temporal signal profiles from these connected areas (Friston et al., 1995). Correlation maps for each participant were obtained from seed-to-voxel connectivity measurements between central, mid-peripheral, and far-peripheral ROIs within the primary visual cortex (V1) to each voxel in the brain (Fig. 3). The resulting correlation coefficient maps were converted to z-score maps using Fisher's z transform. Fischer's transformed z-score maps were projected onto the individual cortical surface from 1 mm below the white/gray matter boundary using Freesurfer's mri_vol2surf command. We compared difference maps by paired, two-tailed *t*-test using Freesurfer's mri_glmfit function to test the functional connectivity differences.

2.5.3.   Diffusion-weighted image preprocessing—The HCP minimal preprocessing pipeline was used to correct B_0 and eddy current distortions (Andersson et al., 2003; Andersson and Sotiropoulos, 2015, 2016; Glasser et al., 2013, 2016; Sotiropoulos et al., 2013). Further, we performed DWI data preprocessing using the FMRIB's Diffusion

Toolbox (FDT v3.0) using GPU for the acceleration of processing (graphics processing unit) (Hernández et al., 2013; Robinson et al., 2018). We estimated the distribution of diffusion parameters using Markov Chain Monte Carlo sampling for each voxel, allowing for crossing fiber orientations (Behrens et al., 2007).

2.5.4.   Tractography—The results from our previous study on functional connectivity, replicated here, led to the hypothesis that structural connections from central vs. peripheral regions would differ between the FPN, CON, and DMN. Thus, we used these network regions as seeds in probabilistic tractography performed by FMRIB's Diffusion Toolbox (FDT) (Hernandez-Fernandez et al., 2019) and used the V1 ROIs as targets. For each seed voxel, we calculated 10,000 streamlines (along with default settings of maximum steps: 2000, step length: 0.5 mm, curvature threshold: 0.2) and separate samples of the voxelwise diffusion distribution. A distance correction and loop-check, which prevents circular pathways, were applied. The tractography then resulted in each voxel within the seed ROI containing the number of streamlines that reached the target (V1 region) from that voxel. We performed tracking in individual diffusion space. We transformed seed and target regions into diffusion space for tractography analysis, and then we transformed tractography results into individual anatomical Freesurfer space for visualization. Surface maps of the track termination probabilities were smoothed using a 2 mm FWHM Gaussian filter and averaged across all subjects.

We transformed track frequencies (number of streamlines that reached the target) into track probabilities (likelihood of a track reaching the target) by dividing the log-scaled track frequency by the maximum log-scaled track frequency (Beer et al., 2011; Wirth et al., 2018). These calculated track probabilities are referred to throughout the paper as "p-track". Track probabilities mitigate possible biases arising from size differences of seeds (Smith et al., 2018; Wirth et al., 2018). Track probabilities were projected onto the individual cortical surface from 1 mm below the white/gray matter boundary using Freesurfer's mri_vol2surf command (Beer et al., 2011; Wirth et al., 2018). Surface maps of the track termination probabilities were smoothed using a 2 mm FWHM Gaussian filter and averaged across all subjects.

After a comparison between functional and structural connectivity (Fig. 7), we performed a deterministic tractography approach to be able to view the pathway connecting central V1 and the frontal portion of the multi-modality overlapping region using DSI studio and a HCP 900-subject release template (Yeh and Tseng, 2011; Yeh et al., 2013, 2018a, 2018b)

2.5.5.   Tractography analysis—To statistically test patterns of structural connections, we compared the central and far-peripheral eccentricity segments of V1 connectivity patterns within the FPN, CON, and DMN. Differences in track probabilities corresponding to V1 eccentricity segment connections were compared by paired, two-tailed t-test (using Freesurfer's mri_glmfit with a one-sample group mean test) (Fig. 5).

2.5.6.   Comparison of functional and structural connectivity—The spatial permutation approach to testing the overlap between two spatial brain maps developed by Alexander-Bloch and colleagues generates a null model for the overlap between spatial brain

maps by randomly rotating the surface maps (Alexander-Bloch et al., 2018). To compare structural and functional connectivity patterns of central vs. far-peripheral V1, we used the spatial permutation approach to compare structural and functional maps within the FPN, CON, DMN, and across all 3 of the networks together. The functional map used in these analyses were the functional connectivity differences between central and far-peripheral V1 ROIs, thresholded at $p < .001$ (See Fig. 4). The structural map used in these analyses was the structural connectivity differences between central and far-peripheral V1 ROIs thresholded at $p < 0.001$ (See Fig. 6). We used a p-value threshold of $p < .001$ to include only those vertices with confidence in the differences' direction.

2.5.7. Correspondence between functional networks and multi-modal connectivity patterns—We defined a multi-modal connectivity pattern as the voxels where connectivity for central V1 was greater than far-peripheral V1 (t-test, threshold $p < .001$) in *both* the structural and functional data (Fig. 7). We tested the spatial overlap between this multi-modal connectivity pattern to each of the functional network ROIs (FPN, CON, DMN) using the spatial permutation approach (Alexander-Bloch et al., 2018). We then compared the correlations of tests of overlap and functional network ROIs to assess if the pattern was more highly correlated to FPN than CON and DMN using cocor function (Diedenhofen and Musch, 2015).

3. Results

We hypothesized that the connectivity between the eccentricity segments of the primary visual cortex (V1) and functional networks (i.e., FPN, CON, DMN) differs in both structural and functional connections.

3.1. Functional connections to V1 depend on eccentricity

We compared the whole-brain functional connectivity patterns of each segment of V1- central, mid-peripheral, and far-peripheral. The t-test comparing functional connectivity to different eccentricity segments in V1 revealed significant effects ($p < .001$) in brain regions belonging to FPN, CON, and DMN functional networks (Fig. 3). Notably, central representing V1 was preferentially connected (over mid-peripheral and far-peripheral V1) to regions associated with the FPN, including the mid orbitofrontal and inferior parietal regions of the FPN (Fig. 3, left). Mid and far-peripheral representing V1 were not preferentially connected (over central V1) to specific networks (Baldassano et al., 2016). This finding of patterns of voxels with preferential connectivity to central V1 is similar to those found in a previous publication from our lab (Griffis et al., 2017). However, the patterns of voxels with preferential connectivity to mid-peripheral and far-peripheral V1 were not as distinct from each other as in the previous dataset (Fig. 3 middle and right). Thus, in this paper, we focus on distinctions between centrally representing portions of V1 to far-peripheral portions of V1.

Due to indications of similarity between patterns of functional connectivity of central V1 and the FPN (from previous data in Griffis et al., 2017), we directly compared central and peripheral V1 functional connections to FPN. We performed pairwise statistical comparisons (t-test) of functional connections between central vs. far-peripheral eccentricity segments

of V1 and the FPN (Fig. 4). Results indicate that, like our initial functional connectivity findings (Fig. 3), there are preferential connections between central V1 and the inferior frontal gyrus compared to far-peripheral V1 (Fig. 4). This inferior frontal gyrus region aligns well with the anterior portion of the FPN as defined by Yeo, but interestingly, it does expand somewhat beyond that border into more inferior parts of the Inferior Frontal Gyrus (IFG). Like the FPN, the IFG is related to attention and control (Baldauf and Desimone, 2014; Chong et al., 2008; Fassbender et al., 2004; Hampshire et al., 2010; Swick et al., 2008, 2011).

3.2. Structural connectivity eccentricity differences

Next, we investigated similar comparisons between central and far-peripheral V1 in a different modality-structural connections. A *t*-test comparing the structural connections of central and far-peripheral V1 revealed significant effects ($p < .001$) in brain regions belonging to FPN, CON, and DMN functional networks (Fig. 5). We chose these three networks to compare to functional connectivity findings from Fig. 3.

Notably, central representing V1 was preferentially connected (over far-peripheral V1) to regions associated with the FPN, including the mid orbitofrontal and inferior parietal regions of the FPN, as well as lateral portions of the DMN, and the insular portion of the CON. In contrast, far-peripheral representing V1 was preferentially connected (over central V1) to medial portions of the DMN (Fig. 5). To follow up on functional connectivity findings (Fig. 4) and to show more clearly the specific region within the FPN, the findings of Fig. 5 have been masked for only the FPN in Fig. 6. Results indicate that, like our functional connectivity findings, there are also preferential structural connections between central V1 and the FPN compared to far-peripheral V1 (Fig. 6).

3.3. Comparison of functional and structural connectivity patterns

To compare the patterns of functional and structural connections, we tested the spatial overlap of a map of structural connectivity differences between central vs. far-peripheral connectivity where central V1 connections were stronger than peripheral connections to the analogous map of functional differences in the same set of vertices. Vertices included in this analysis included all vertices within FPN, CON, and DMN combined, as these were the vertices with information about structural connections to V1 in our analysis. The spatial overlap between structural and functional connectivity patterns was statistically significant ($r = 0.302$, $p = .002$). We then examined each of the three networks individually for how similar the structural and functional connectivity findings were within the vertices of each functional network. Within the FPN, the spatial overlap between structural and functional connectivity patterns was statistically significant ($r = 0.431$, $p = <0.00001$). Within the CON, the spatial overlap between structural and functional connectivity patterns was statistically significant ($r = 0.097$, $p = .006$). Within the DMN, the spatial overlap between structural and functional connectivity patterns was statistically significant ($r = 0.366$, $p = <0.0001$). These relationships indicate that the overall pattern of vertices with stronger connections to central V1 than peripheral V1 is significantly consistent across structural and functional modalities, a result consistent with prior work (Honey et al., 2009).

3.4. Correspondence between functional networks and multi-modal connectivity patterns

Fig. 7 shows regions where the central V1 segment had higher connectivity than the far-peripheral V1 segment in structural and functional comparisons. These regions include lateral frontal portions of the FPN, and small portions of other networks show overlap between the modalities (including the IFG portions of the DMN as defined from the Yeo et al., 2011 atlas in Fig. 3).

We calculated the spatial overlap between multi-modal regions of central dominance (as shown in Fig. 7) and functional networks (FPN, DMN, CON). The spatial overlap between the FPN and the multi-modal overlap was statistically significant ($r = 0.4543$, $p = <0.0001$), DMN was statistically significant ($r = 0.360$, $p = <0.0001$), and CON was not statistically significant ($r = 0.1613$, $p=.089$). Comparison of these correlations using Fisher's Z test to compare correlations (Diedenhofen and Musch, 2015) indicated that the correlation was higher between FPN and the overlapping regions between structural and functional connectivity than the correlation between either CON or DMN and the overlapping regions ($p<.0001$).

3.5. Correspondence of structural connectivity patterns to the Inferior Fronto-Occipital Fasciculus (IFOF)

After investigating the overlap between functional and structural connectivity patterns (Fig. 7), we isolated the frontal pole regions and performed deterministic tractography. Fig. 8 shows the resulting tractography between central V1 and the frontal regions identified from Fig. 7. Upon visual inspection, the tracks identified were very similar to a major white matter pathway, the IFOF (see Fig. 8, D); therefore, Fig. 8 displays overlapping IFOF (blue) and the tractography results (red).

4. Discussion

Our goal was to better understand the brain network basis for interactions between sensory and higher-order information, especially how this differs between central vs. peripheral vision. Understanding the structural and functional underpinnings of these interactions is essential for understanding the processing differences between central and peripheral vision and for future work examining the plasticity of these systems.

Our approach compared structural and functional connections among different retinotopic eccentricities within V1 and large-scale functional networks (Fronto-Parietal Network (FPN), Cingulo-Opercular Network (CON), Default Mode Network (DMN)). Our results indicated that different visual eccentricities have different connectivity patterns to the rest of the brain, consistent with our previous data (Griffis et al., 2017) and data from other analyses (Buckner and Yeo, 2014). The present functional connectivity analyses replicated and extended previous findings on patterns of preferential connections between the central V1 eccentricity segment and the FPN (Griffis et al., 2017). Our structural connectivity analyses furthered the field's understanding of the relationship between V1 and functional networks by describing the retinotopic pattern of structural connections. A comparison between structure and function showed moderate agreement, indicating that some direct

structural connections likely mediate the functional connections. Further, the overlap of structural and functional findings (Fig. 7) indicated the lateral frontal portions of the FPN and other nearby regions also responsible for attention and control (Inferior frontal gyrus (IFG)) made up more of the overlapping regions than the CON or DMN. This lateral frontal portion of the FPN is connected to central V1 via the IFOF (Fig. 8).

The present study found differences between the connection patterns of central and peripheral representations in V1. Since central and peripheral representations are still part of the same V1 cortical area, we would expect similarities in their connectivity patterns. Our results indicate that eccentricity differences in connection strength exist and are consistent with previously reported differences in information processing central and peripheral visual information. Central vision appears to be under more substantial top-down attentional control than peripheral vision (Chen and Treisman, 2008; Lu et al., 2002; Zhaoping, 2017). For example, stimuli presented within the peripheral visual field are more challenging to ignore than stimuli presented within the central visual field (Chen and Treisman, 2008). The current work suggests that this distinction may come from anatomical relationships to attentional networks.

4.1. Functional connectivity

Our findings are consistent with prior work, specifically, preferential connections between central representing segments of V1 and regions belonging to the FPN (Griffis et al., 2017). These results suggest that frontal areas influence cognitive control mechanisms and primary visual processing areas, specifically central V1. On the other hand, the mid- peripheral and far-peripheral regions seemed to be preferentially connected more broadly across the cortex, with the specific exclusion of the FPN regions. The data provide further evidence to support the hypothesis of eccentricity-dependent preferential connectivity of V1 to higher-order brain networks. One contribution in describing this connectivity is to extend previous work by Griffis et al., 2017, into a much larger dataset that was collected without fixation at rest, thereby improving the generalizability of the findings.

The patterns of connectivity for the mid- and far- peripheral regions (Fig. 3) were similar to each other and both differed from central V1 connectivity. This result suggests that the strongest retinotopic differences in V1 connectivity are rooted in the distinction between foveal and peripheral eccentricities. Using slightly different methods (an analysis of variance across all V1 ROIs, smaller V1 ROIs, fewer participants, resting during a fixation task) Griffis et al. (2017) obtained a similar result, but also observed modestly sized differences between mid and far peripheral V1 which we do not observe here. Further work is needed to identify what factors might lead to this difference.

4.2. Structural connectivity

Finding preferential structural connections between frontal regions to central V1 is consistent with our functional connectivity findings. These results support our hypothesis, based on functional connectivity findings, that the connections between V1 and brain regions associated with attentional control depend on eccentricity. As previously discussed, Markov et al. (2014) investigated direct structural connections in the macaque brain and

found weak long-range connections between V1 and regions that may correspond to the human FPN. These connections were projections *from* V1 to frontal and parietal regions (areas F5, 81, and 7A) rather than projecting *to* V1. These results could indicate that the structural connections observed here are bottom-up connections that provide visual information to direct cognitive control within the FPN. However, previous work in macaques has not found major white matter tracts connecting the occipital lobe to the frontal lobe (Takemura et al., 2017). Further, the attention system of the macaque is different from that in humans (Patel et al., 2015). Thus, the prior macaque literature provides limited insight into the structural connections between V1 and FPN in humans, so the direction of these connections is still unclear. Although diffusion tractography methods can conflate crossing fibers, tractography showed strikingly similar effects to our functional connectivity results, bolstering the plausibility of an interpretation of a direct connection between lateral frontal regions to V1. Describing this connectivity extends the knowledge of functional connectivity between V1 and functional networks and improves our understanding of the structural underpinnings of these functional connections.

4.3. Overlap between structural and functional connections and their relationship to functional networks

Structural connectivity patterns and functional connectivity patterns showed correspondence. Because diffusion tractography is typically interpreted as a direct structural connection, the functional connections between regions that also showed a structural connection likely reflect (at least in part) direct structural connections. These regions that showed centrally-weighted structural and functional connections are shown in Fig. 7 and include the inferior frontal gyrus.

A direct, long-range connection between IFG and central vision representations in V1 may be related to the importance of speed in attentional control. For example, visual information needs to be processed quickly to impact attention selection. Thus, attentional control from the FPN to central vision representations in V1 would be improved by direct structural connections. Direct structural connections would also improve the processing of central vision information in FPN circuits. A large body of work supports top-down and bottom-up effects on visual processing (Gandhi et al., 1999; Somers et al., 1999; Tootell et al., 1998; Yeshurun and Carrasco, 1998; Zhaoping, 2017). The present study contributes to this field by demonstrating the eccentricity-dependent nature of the relationship between V1 and higher-order brain regions and the major white matter pathway, IFOF, that connects these regions.

4.4. Relationship between central vision processing and attention

Complex biological systems are often driven by separate control mechanisms with distinct functional properties (Dosenbach et al., 2008). During cognitive operations, information processing appears to rely on brain areas' dynamic interaction as large-scale neural networks including FPN, CON, and DMN. FPN supports executive functions by initiating and adjusting top-down control (Dosenbach et al., 2008). The CON supports salience-related functions and provides stable control over entire task epochs. The suppression of DMN is critical for goal-directed cognitive processes (Spreng et al., 2010). Cooperation among

these top-down control systems of the brain is necessary for controlling attention, working memory, decision making, and other high-level cognitive operations (Hellyer et al., 2014; Keller et al., 2015; Raichle, 2015; Ray et al., 2020; Spreng, 2012; Vincent et al., 2008).

FPN includes regions such as the intraparietal sulcus that play an essential role in goal-directed cognitive functions Spreng et al., 2010) and both spatial and non-spatial visual attention (Giesbrecht et al., 2003; Scolari et al., 2015). The role of central vision in visual processing and object recognition and the need to inhibit distractors in the visual field could (speculatively) be an evolutionary reason central vision representations are preferentially connected to attention regions, including the FPN. Contributions from high-order cognitive areas, like the FPN, help the brain decide which visual areas will be prioritized for visual attention (Scolari et al., 2015).

4.5. Limitations and future directions

Our study has several methodological limitations that we will discuss here. Our study used only healthy young adults from the HCP dataset, which could influence our findings' generalizability. Future work should include individuals from across the lifespan.

The task participants completed during the HCP protocol was quite distinct from the previous dataset's task (Griffis et al., 2017). Here, participants rested quietly, and though their instruction was to keep eyes open, no one assessed if the participants' eyes were open or closed. In contrast, the Griffis dataset included data from the rest period between blocks of a task, and eye position and lid opening were confirmed via eye-tracking. The fact that these data closely follow each other extends the possible interpretations of the original dataset: the distinction between peripheral and central V1 connectivity generalizes to a new task context.

It should also be acknowledged that functional connectivity can be influenced by attention (Gratton et al., 2018; Griffis et al., 2015; Salehi et al., 2020). In both the work by Griffis et al. (2017) and the current study's resting-state scan, a fixation cross presented on a screen at the end of the bore, and participants were scanned while inside the MRI bore. Participants may therefore have been allocating more attention toward the visual space in the center (the static screen, subtending roughly 15° visual angle) than the periphery (the bore). However, the fact that we observed complementary effects in the structural data indicates that these data are likely not due to transient states of attention and are likely to represent the biological organization.

We acknowledge that large veins near posterior occipital cortex area V1 could impact our functional connectivity measurements in this area (Winawer et al., 2010). However, we performed extensive preprocessing to reduce the impact of vessels on the results. In addition, the voxel size of our resting state scan is small (2 mm isotropic); this higher resolution should mitigate contributions from nearby veins due to partial voluming effects (Schira et al., 2009).

Functional connectivity strengths between V1 to the lateral frontal cortex are on the order of $r = 0.1$ (Fig. 4). While statistically significant ($p < .001$), the magnitudes of these functional

connections are not as large as connections from V1 to other areas, for example, other portions of the occipital lobe. Functional connectivity magnitudes are always influenced by the preprocessing done to obtain them. In this case, we regressed out the mean signal and regressed out white matter and CSF. While this practice decreases the mean correlation strength (Shirer et al., 2015; Weissenbacher et al., 2009), it also improves across-subject reliability (Burgess et al., 2016). The debate about this practice, now a decade long, has focused on the interpretability of negative correlations, which we do not do here; our inferences are based on differences in correlations across brain areas.

DWI-based tractography produces similar results to tracer methods (Donahue et al., 2016); however, probabilistic tractography indirectly traces axon bundles by modeling the path of most restricted water movement and then estimating white matter tracts. Fibers that cross, fan, or converge pose problems for accurately estimating white matter tracts (Johansen-Berg and Rushworth, 2009). One way to improve track estimation is by modeling multiple angular compartments (e.g., ball-and-stick model) and using greater than 30 diffusion directions (i.e., 95, 96, and 97 directions in the present study), both of which were used in the present study (Behrens et al., 2007). Connections described in tractography are non-directional in that no determination of the direction of signaling is acquired. Therefore, the current study cannot interpret the direction (top-down versus bottom-up processing) of the described connections outside of the context of prior tracer studies.

Although the present tractography and functional connectivity analyzes aim to measure connections between eccentricity segments of V1 and functional networks, they are inherently different modalities, including but not limited to differences in the measurement of direct and indirect connections between regions. Tractography derived from diffusion-weighted imaging identifies direct connections (Forkel et al., 2014), whereas functional connectivity identifies both direct and indirect connections. Therefore, the comparison between them is limited in scope. Since tractography describes direct connections between brain regions, inconsistencies where functional connectivity is present but structural connectivity is not, could be due to multi-synaptic, indirect connections (Honey et al., 2009; Vázquez-Rodríguez et al., 2019). Measuring both structural and functional connectivity provides valuable information to understand the relationship between brain regions that cannot be derived from one modality alone.

Future work could help determine the direction of the observed connections and further describe the complexity of direct and indirect connections between V1 and functional networks and examine extrastriate regions that are retinotopically mapped. While we only studied participants with healthy vision, future work should include participants with low vision to investigate possible connectivity changes related to vision loss. This work could serve as a baseline for these low vision studies. Future research could also help inform the plasticity of the described connections in the context of visual training and vision loss.

4.6. Conclusions

There is a reliable preference for central representations in V1 to be more strongly connected to the frontoparietal network than peripheral visual representations. This is particularly true for the lateral frontal portions of that network and the Inferior Frontal

Gyrus and is true for structural as well as functional connections. This implies that the functional relationship between central V1 and frontal regions is built, at least in part, upon direct, long-distance connections in the IFOF. Understanding how V1 is functionally and structurally connected to higher-order brain areas contributes to our understanding of how the human brain processes visual information and forms a baseline for understanding any modifications in processing that might occur with training or experience.

In summary, the work's main contribution is a greater understanding of higher-order functional networks' connectivity to the primary visual cortex (V1). Centrally-representing portions of V1 are connected to some frontal cortical regions, including portions of the FPN, both functionally and structurally. The lateral frontal regions where connection differences overlap between structural and functional data have been associated with attention in previous work. This suggests that the central representations of V1 are more tightly coupled to some brain regions involved in attention and cognitive control. Understanding how V1 is functionally and structurally connected to higher-order brain areas contributes to our understanding of how the human brain processes visual information and forms a baseline for understanding any modifications in processing that might occur with training or experience.

Supplementary Material

Refer to Web version on PubMed Central for supplementary material.

Acknowledgments

References

Adachi Y, Osada T, Sporns O, Watanabe T, Matsui T, Miyamoto K, Miyashita Y, 2012. Functional connectivity between anatomically unconnected areas is shaped by collective network-level effects in the macaque cortex. Cereb. Cortex22 (7), 1586–1592. [PubMed: 21893683]

Alexander-Bloch AF, Shou H, Liu S, Satterthwaite TD, Glahn DC, Shinohara RT, Vandekar SN, et al., 2018. On testing for spatial correspondence between maps of human brain structure and function. Neuroimage178, 540–551. [PubMed: 29860082]

Andersen RA, Asanuma C, Essick G, Siegel RM, 1990. Corticocortical connections of anatomically and physiologically defined subdivisions within the inferior parietal lobule. J. Comp. Neurol296 (1), 65–113. [PubMed: 2358530]

Andersson JLR, Skare S, Ashburner J, 2003. How to correct susceptibility distortions in spin-echo echo-planar images: application to diffusion tensor imaging. Neuroimage20 (2), 870–888. [PubMed: 14568458]

Andersson JLR, Sotiropoulos SN, 2015. Non-parametric representation and prediction of single- and multi-shell diffusion-weighted MRI data using Gaussian processes. Neuroimage122, 166–176. [PubMed: 26236030]

Andersson JLR, Sotiropoulos SN, 2016. An integrated approach to correction for off-resonance effects and subject movement in diffusion MR imaging. Neuroimage125, 1063–1078. [PubMed: 26481672]

Azzopardi P, Cowey A, 1993. Preferential representation of the fovea in the primary visual cortex. Nature361 (6414), 719–721. [PubMed: 7680108]

Baldassano C, Fei-Fei L, Beck DM, 2016. Pinpointing the peripheral bias in neural scene-processing networks during natural viewing. J. Vis16 (2), 9.

Baldauf D, Desimone R, 2014. Neural mechanisms of object-based attention. Science344 (6182), 424–427. [PubMed: 24763592]

Beer AL, Plank T, Greenlee MW, 2011. Diffusion tensor imaging shows white matter tracts between human auditory and visual cortex. Exp. Brain Res213 (2–3), 299–308. [PubMed: 21573953]

Behrens TEJ, Johansen-Berg H, Jbabdi S, Rushworth MFS, Woolrich MW, 2007. Probabilistic diffusion tractography with multiple fibre orientations: what can we gain?Neuroimage34 (1), 144–155. [PubMed: 17070705]

Benson NC, Butt OH, Brainard DH, Aguirre GK, 2014. Correction of distortion in flattened representations of the cortical surface allows prediction of V1-V3 functional organization from anatomy. PLoS Comput. Biol10 (3), e1003538. [PubMed: 24676149]

Benson NC, Butt OH, Datta R, Radoeva PD, Brainard DH, Aguirre GK, 2012. The retinotopic organization of striate cortex is well predicted by surface topology. Curr. Biol22 (21), 2081–2085. [PubMed: 23041195]

Benson NC, Winawer J, 2018. Bayesian analysis of retinotopic maps. Elife7 (e40224). [PubMed: 30520736]

Binder JR, 2012. Task-induced deactivation and the "resting" state. Neuroimage62 (2), 1086–1091, [PubMed: 21979380]

Buckner RL, Yeo BTT, 2014. Borders, map clusters, and supra-areal organization in visual cortex. Neuroimage93, 292–297Pt 2. [PubMed: 24374078]

Burgess GC, Kandala S, Nolan D, Laumann TO, Power JD, Adeyemo B, Harms MP, et al., 2016. Evaluation of denoising strategies to address motion-correlated artifacts in resting-state functional magnetic resonance imaging data from the human connectome project. Brain Connect. 6 (9), 669–680. [PubMed: 27571276]

Burge WK, Griffis JC, Nenert R, Elkhetali A, DeCarlo DK, ver Hoef LW, Ross LA, et al. , 2016. Cortical thickness in human V1 associated with central vision loss. Sci. Rep 6, 23268. [PubMed: 27009536]

Carp J, 2013. Optimizing the order of operations for movement scrubbing: comment on Power et alet al.Neuroimage76, 436–438. [PubMed: 22227884]

Casarsa De Azevedo FA, 2019. Functional Neuroimaging of Resting-State and Stimulus–Driven Networks in the Macaque Brain. Universität Tübingen.

Chen Z, Treisman A, 2008. Distractor inhibition is more effective at a central than at a peripheral location. Percept. Psychophys70 (6), 1081–1091. [PubMed: 18717393]

Chong TTJ, Williams MA, Cunnington R, Mattingley JB, 2008. Selective attention modulates inferior frontal gyrus activity during action observation. Neuroimage40 (1), 298–307. [PubMed: 18178107]

Coste CP, Kleinschmidt A, 2016. Cingulo-opercular network activity maintains alertness. Neuroimage128, 264–272. [PubMed: 26801604]

Davis SW, Dennis NA, Buchler NG, White LE, Madden DJ, Cabeza R, 2009. Assessing the effects of age on long white matter tracts using diffusion tensor tractography. Neuroimage46 (2), 530–541. [PubMed: 19385018]

Diedenhofen B, Musch J, 2015. cocor: a comprehensive solution for the statistical comparison of correlations. PLoS ONE10 (3), e0121945. [PubMed: 25835001]

Donahue CJ, Sotiropoulos SN, Jbabdi S, Hernandez-Fernandez M, Behrens TE, Dyrby TB, Coalson T, et al., 2016. Using diffusion tractography to predict cortical connection strength and distance: a quantitative comparison with tracers in the monkey. J. Neurosci36 (25), 6758–6770. [PubMed: 27335406]

Dosenbach NUF, Fair DA, Cohen AL, Schlaggar BL, Petersen SE, 2008. A dual-networks architecture of top-down control. Trends Cogn. Sci12 (3), 99–105 (Regul. Ed.). [PubMed: 18262825]

Duncan RO, Sample PA, Weinreb RN, Bowd C, Zangwill LM, 2007. Retinotopic organization of primary visual cortex in glaucoma: comparing fMRI measurements of cortical function with visual field loss. Prog. Retin. Eye Res26 (1), 38–56. [PubMed: 17126063]

Engel SA, Glover GH, Wandell BA, 1997. Retinotopic organization in human visual cortex and the spatial precision of functional MRI. Cereb. Cortex7 (2), 181–192. [PubMed: 9087826]

Fassbender C, Murphy K, Foxe JJ, Wylie GR, Javitt DC, Robertson IH, Garavan H, 2004. A topography of executive functions and their interactions revealed by functional magnetic resonance imaging. Brain Res. Cogn. Brain Res20 (2), 132–143. [PubMed: 15183386]

Fischl B, 2012. FreeSurfer. Neuroimage62 (2), 774–781. [PubMed: 22248573]

Forkel SJ, Thiebaut de Schotten M, Kawadler JM, Dell'Acqua F, Danek A, Catani M, 2014. The anatomy of fronto-occipital connections from early blunt dissections to contemporary tractography. Cortex56, 73–84. [PubMed: 23137651]

Fox PT, Miezin FM, Allman JM, Van Essen DC, Raichle ME, 1987. Retinotopic organization of human visual cortex mapped with positron-emission tomography. J. Neurosci7 (3), 913–922. [PubMed: 3494107]

Friston K, Holmes A, Poline JB, Frith C, Frackowiak R, 1995. Statistical parametric maps in functional imaging: {A} general linear approach. Hum. Brain Map2 (081), 189–210.

Furl N, 2015. Structural and effective connectivity reveals potential network-based influences on category-sensitive visual areas. Front. Hum. Neurosci9, 253. [PubMed: 25999841]

Gandhi SP, Heeger DJ, Boynton GM, 1999. Spatial attention affects brain activity in human primary visual cortex. Proc. Natl. Acad. Sci. U.S.A96 (6), 3314–3319. [PubMed: 10077681]

Gazzaley A, Rissman J, Cooney J, Rutman A, Seibert T, Clapp W, D'Esposito M, 2007. Functional interactions between prefrontal and visual association cortex contribute to top-down modulation of visual processing. Cereb. Cortex17 (Suppl 1), i125–i135. [PubMed: 17725995]

Gerlach KD, Spreng RN, Gilmore AW, Schacter DL, 2011. Solving future problems: default network and executive activity associated with goal-directed mental simulations. Neuroimage55 (4), 1816–1824. [PubMed: 21256228]

Giesbrecht B, Woldorff MG, Song AW, Mangun GR, 2003. Neural mechanisms of top-down control during spatial and feature attention. Neuroimage19 (3), 496–512, [PubMed: 12880783]

Gilbert CD, Li W, 2013. Top-down influences on visual processing. Nat. Rev. Neurosci14 (5), 350–363. [PubMed: 23595013]

Glasser MF, Smith SM, Marcus DS, Andersson JLR, Auerbach EJ, Behrens TEJ, Coalson TS, et al., 2016. The human connectome project's neuroimaging approach. Nat. Neurosci19 (9), 1175–1187. [PubMed: 27571196]

Glasser MF, Sotiropoulos SN, Wilson JA, Coalson TS, Fischl B, Andersson JL, Xu J, et al., 2013. The minimal preprocessing pipelines for the human connectome project. Neuroimage80, 105–124. [PubMed: 23668970]

Gratton C, Laumann TO, Nielsen AN, Greene DJ, Gordon EM, Gilmore AW, Nelson SM, et al., 2018. Functional brain networks are dominated by stable group and individual factors, not cognitive or daily variation. Neuron98 (2), 439–452 e5. [PubMed: 29673485]

Griffis JC, Elkhetali AS, Burge WK, Chen RH, Bowman AD, Szaflarski JP, Visscher KM, 2017. Retinotopic patterns of functional connectivity between V1 and large-scale brain networks during resting fixation. Neuroimage146, 1071–1083, [PubMed: 27554527]

Griffis JC, Elkhetali AS, Burge WK, Chen RH, Visscher KM, 2015. Retinotopic patterns of background connectivity between V1 and fronto-parietal cortex are modulated by task demands. Front. Hum. Neurosci9, 338. [PubMed: 26106320]

Hampshire A, Chamberlain SR, Monti MM, Duncan J, Owen AM, 2010. The role of the right inferior frontal gyrus: inhibition and attentional control. Neuroimage50 (3), 1313–1319. [PubMed: 20056157]

Harvey BM, Dumoulin SO, 2011. The relationship between cortical magnification factor and population receptive field size in human visual cortex: constancies in cortical architecture. J. Neurosci31 (38), 13604–13612. [PubMed: 21940451]

Hellyer PJ, Shanahan M, Scott G, Wise RJS, Sharp DJ, Leech R, 2014. The control of global brain dynamics: opposing actions of frontoparietal control and default mode networks on attention. J. Neurosci34 (2), 451–461. [PubMed: 24403145]

Hernandez-Fernandez M, Reguly I, Jbabdi S, Giles M, Smith S, Sotiropoulos SN, 2019. Using GPUs to accelerate computational diffusion MRI: from microstructure estimation to tractography and connectomes. Neuroimage188, 598–615. [PubMed: 30537563]

Hernández M, Guerrero GD, Cecilia JM, García JM, Inuggi A, Jbabdi S, Behrens TEJ, et al., 2013. Accelerating fibre orientation estimation from diffusion weighted magnetic resonance imaging using GPUs. PLoS ONE8 (4), e61892. [PubMed: 23658616]

Hinds O, Polimeni JR, Rajendran N, Balasubramanian M, Amunts K, Zilles K, Schwartz EL, et al., 2009. Locating the functional and anatomical boundaries of human primary visual cortex. Neuroimage46 (4), 915–922. [PubMed: 19328238]

Hinds OP, Rajendran N, Polimeni JR, Augustinack JC, Wiggins G, Wald LL, Diana Rosas H, et al., 2008. Accurate prediction of V1 location from cortical folds in a surface coordinate system. Neuroimage39 (4), 1585–1599. [PubMed: 18055222]

Honey CJ, Sporns O, Cammoun L, Gigandet X, Thiran JP, Meuli R, Hagmann P, 2009. Predicting human resting-state functional connectivity from structural connectivity. Proc. Natl. Acad. Sci. U.S.A106 (6), 2035–2040. [PubMed: 19188601]

Horton JC, Hoyt WF, 1991. The representation of the visual field in human striate cortex. A revision of the classic Holmes map. Arch. Ophthalmol109 (6), 816–824. [PubMed: 2043069]

Hubel DH, Wiesel TN, 1974. Uniformity of monkey striate cortex: a parallel relationship between field size, scatter, and magnification factor. J. Comp. Neurol158 (3), 295–305. [PubMed: 4436457]

Jbabdi S, Johansen-Berg H, 2011. Tractography: where do we go from here?Brain Connect. 1 (3), 169–183. [PubMed: 22433046]

Jenkinson M, Beckmann CF, Behrens TE, Woolrich MW, Smith SM, 2012. FSL.. Neuroimage62 (2), 782–790. [PubMed: 21979382]

Jenkinson M, Bannister P, Brady M, Smith S, 2002. Improved optimization for the robust and accurate linear registration and motion correction of brain images. Neuroimage17 (2), 825–841. [PubMed: 12377157]

Johansen-Berg H, Rushworth MFS, 2009. Using diffusion imaging to study human connectional anatomy. Annu. Rev. Neurosci32, 75–94. [PubMed: 19400718]

Katsuki F, Constantinidis C, 2014. Bottom-up and top-down attention: different processes and overlapping neural systems. The Neuroscientist20 (5), 509–521. [PubMed: 24362813]

Keller JB, Hedden T, Thompson TW, Anteraper SA, Gabrieli JDE, Whitfield-Gabrieli S, 2015. Resting-state anticorrelations between medial and lateral prefrontal cortex: association with working memory, aging, and individual differences. Cortex64, 271–280. [PubMed: 25562175]

Larson AM, Loschky LC, 2009. The contributions of central versus peripheral vision to scene gist recognition. J. Vis9 (10), 1–16.

Levi DM, Klein SA, Aitsebaomo AP, 1985. Vernier acuity, crowding and cortical magnification. Vis. Res25 (7), 963–977. [PubMed: 4049746]

Levi DM, Klein SA, Wang H, 1994. Discrimination of position and contrast in amblyopic and peripheral vision. Vision Res. 34 (24), 3293–3313. [PubMed: 7863615]

Li Z, 2002. A saliency map in primary visual cortex. Trends Cogn. Sci6 (1), 9–16 (Regul. Ed.). [PubMed: 11849610]

Lu ZL, Lesmes LA, Dosher BA, 2002. Spatial attention excludes external noise at the target location. J. Vis2 (4), 312–323. [PubMed: 12678581]

Lysakowski A, Standage GP, Benevento LA, 1988. An investigation of collateral projections of the dorsal lateral geniculate nucleus and other subcortical structures to cortical areas V1 and V4 in the macaque monkey: a double label retrograde tracer study. Exp. Brain Res69 (3), 651–661. [PubMed: 2836233]

Maier-Hein KH, Neher PF, Houde JC, Côté MA, Garyfallidis E, Zhong J, Chamberland M, et al., 2017. The challenge of mapping the human connectome based on diffusion tractography. Nat. Commun8 (1), 1349. [PubMed: 29116093]

Mantini D, Corbetta M, Perrucci MG, Romani GL, Del Gratta C, 2009. Large-scale brain networks account for sustained and transient activity during target detection. Neuroimage44 (1), 265–274. [PubMed: 18793734]

Markov NT, Ercsey-Ravasz MM, Ribeiro Gomes AR, Lamy C, Magrou L, Vezoli J, Misery P, et al., 2014. A weighted and directed interareal connectivity matrix for macaque cerebral cortex. Cereb. Cortex24 (1), 17–36. [PubMed: 23010748]

McMains S, Kastner S, 2011. Interactions of top-down and bottom-up mechanisms in human visual cortex. J. Neurosci31 (2), 587–597. [PubMed: 21228167]

Neal JW, Pearson RCA, Powell TPS, 1990. The ipsilateral cortico-cortical connections of area 7b, PF, in the parietal and tempral lobes of the monkey. Brain Res. 524 (1), 119–132. [PubMed: 1698108]

Patel GH, Yang D, Jamerson EC, Snyder LH, Corbetta M, Ferrera VP, 2015. Functional evolution of new and expanded attention networks in humans. Proc. Natl. Acad. Sci. U.S.A112 (30), 9454–9459. [PubMed: 26170314]

Pelli DG, Tillman KA, Freeman J, Su M, Berger TD, Majaj NJ, 2007. Crowding and eccentricity determine reading rate. J. Vis7 (2), 1–36.

Power JD, Barnes KA, Snyder AZ, Schlaggar BL, Petersen SE, 2012. Spurious but systematic correlations in functional connectivity MRI networks arise from subject motion. Neuroimage59 (3), 2142–2154. [PubMed: 22019881]

Raichle ME, 2015. The brain's default mode network. Annu. Rev. Neurosci38, 433–447. [PubMed: 25938726]

Ray KL, Ragland JD, MacDonald AW, Gold JM, Silverstein SM, Barch DM, Carter CS, 2020. Dynamic reorganization of the frontal parietal network during cognitive control and episodic memory. Cognitive, Affective, & Behavioral Neuroscience20, 76–90.

Roberts M, Delicato LS, Herrero J, Gieselmann MA, Thiele A, 2007. Attention alters spatial integration in macaque V1 in an eccentricity-dependent manner. Nat. Neurosci10 (11), 1483–1491. [PubMed: 17906622]

Robinson JP, Anthony T, Tripathi R, Sims SA, Visscher KM, Bangalore PV, 2018. Analyzing the Human Connectome Project Datasets using GPUs: the Anatomy of a Science Engagement. In: Proceedings of the Practice and Experience on Advanced Research Computing - PEARC '18 (pp. 1–6). Presented at the the Practice and Experience. New York, New York, USA. ACM Press.

Rosenholtz R, 2016. Capabilities and limitations of peripheral vision. Annu. Rev. Vis. Sci2, 437–457. [PubMed: 28532349]

Salehi M, Greene AS, Karbasi A, Shen X, Scheinost D, Constable RT, 2020. There is no single functional atlas even for a single individual: functional parcel definitions change with task. Neuroimage208, 116366. [PubMed: 31740342]

Schira MM, Tyler CW, Breakspear M, Spehar B, 2009. The foveal confluence in human visual cortex. J. Neurosci29 (28), 9050–9058. [PubMed: 19605642]

Scolari M, Seidl-Rathkopf KN, Kastner S, 2015. Functions of the human frontoparietal attention network: evidence from neuroimaging. Curr. Opin. Behav. Sci1, 32–39. [PubMed: 27398396]

Sestieri C, Shulman GL, Corbetta M, 2010. Attention to memory and the environment: functional specialization and dynamic competition in human posterior parietal cortex. J. Neurosci30 (25), 8445–8456. [PubMed: 20573892]

Shirer WR, Jiang H, Price CM, Ng B, Greicius MD, 2015. Optimization of rs-fMRI pre-processing for enhanced signal-noise separation, test-retest reliability, and group discrimination. Neuroimage117, 67–79, [PubMed: 25987368]

Smith AT, Beer AL, Furlan M, Mars RB, 2018. Connectivity of the cingulate sulcus visual area (csv) in the human cerebral cortex. Cereb. Cortex28 (2), 713–725. [PubMed: 28108496]

Somers DC, Dale AM, Seiffert AE, Tootell RB, 1999. Functional MRI reveals spatially specific attentional modulation in human primary visual cortex. Proc. Natl. Acad. Sci. U.S.A96 (4), 1663–1668. [PubMed: 9990081]

Sotiropoulos SN, Jbabdi S, Xu J, Andersson JL, Moeller S, Auerbach EJ, Glasser MF, et al., 2013. Advances in diffusion MRI acquisition and processing in the Human Connectome Project. Neuroimage80, 125–143. [PubMed: 23702418]

Spreng RN, Stevens WD, Chamberlain JP, Gilmore AW, Schacter DL, 2010. Default network activity, coupled with the frontoparietal control network, supports goal-directed cognition. Neuroimage53 (1), 303–317. [PubMed: 20600998]

Spreng RN, 2012. The fallacy of a "task-negative" network. Front. Psychol3, 145. [PubMed: 22593750]

Swick D, Ashley V, Turken AU, 2008. Left inferior frontal gyrus is critical for response inhibition. BMC Neurosci. 9, 102. [PubMed: 18939997]

Swick D, Ashley V, Turken U, 2011. Are the neural correlates of stopping and not going identical? Quantitative meta-analysis of two response inhibition tasks. Neuroimage56 (3), 1655–1665. [PubMed: 21376819]

Takemura H, Pestilli F, Weiner KS, Keliris GA, Landi SM, Sliwa J, Ye FQ, et al., 2017. Occipital white matter tracts in human and macaque. Cerebral Cortex27 (6), 3346–3359. [PubMed: 28369290]

Tootell RB, Hadjikhani N, Hall EK, Marrett S, Vanduffel W, Vaughan JT, Dale AM, 1998. The retinotopy of visual spatial attention. Neuron21 (6), 1409–1422. [PubMed: 9883733]

Trouilloud A, Kauffmann L, Roux-Sibilon A, Rossel P, Boucart M, Mermillod M, Peyrin C, 2020. Rapid scene categorization: from coarse peripheral vision to fine central vision. Vis. Res170, 60–72. [PubMed: 32259648]

Van Essen David C, Smith SM, Barch DM, Behrens TEJ, Yacoub E, Ugurbil K, Consortium, WU-Minn HCP, 2013. The WU-Minn Human Connectome Project: an overview. Neuroimage80, 62–79. [PubMed: 23684880]

Van Essen DC, Ugurbil K, Auerbach E, Barch D, Behrens TEJ, Bucholz R, Chang A, et al., 2012. The Human Connectome Project: a data acquisition perspective. Neuroimage62 (4), 2222–2231. [PubMed: 22366334]

Vázquez-Rodríguez B, Suárez LE, Markello RD, Shafiei G, Paquola C, Hagmann P, van den Heuvel MP, et al., 2019. Gradients of structure-function tethering across neocortex. Proc. Natl. Acad. Sci. U.S.A116 (42), 21219–21227. [PubMed: 31570622]

Vincent JL, Kahn I, Snyder AZ, Raichle ME, Buckner RL, 2008. Evidence for a frontoparietal control system revealed by intrinsic functional connectivity. J. Neurophysiol100 (6), 3328–3342. [PubMed: 18799601]

Weissenbacher A, Kasess C, Gerstl F, Lanzenberger R, Moser E, Windischberger C, 2009. Correlations and anticorrelations in resting-state functional connectivity MRI: a quantitative comparison of preprocessing strategies. Neuroimage47 (4), 1408–1416. [PubMed: 19442749]

Winawer J, Horiguchi H, Sayres RA, Amano K, Wandell BA, 2010. Mapping hV4 and ventral occipital cortex: the venous eclipse. J. Vis10 (5), 1.

Wirth AM, Frank SM, Greenlee MW, Beer AL, 2018. White matter connectivity of the visual-vestibular cortex examined by diffusion-weighted imaging. Brain Connect. 8 (4), 235–244, [PubMed: 29571264]

Wu Y, Sun D, Wang Y, Wang Y, 2016. Subcomponents and connectivity of the inferior fronto-occipital fasciculus revealed by diffusion spectrum imaging fiber tracking. Front. Neuroanat10, 88. [PubMed: 27721745]

Yeh FC, Panesar S, Barrios J, Fernandes D, Abhinav K, Meola A, Fernandez-Miranda JC, 2018a. Automatic removal of false connections in diffusion MRI tractography using topology-informed pruning (TIP). BioRxiv.

Yeh FC, Panesar S, Fernandes D, Meola A, Yoshino M, Fernandez-Miranda JC, Vettel JM, et al., 2018b. Population-averaged atlas of the macroscale human structural connectome and its network topology. Neuroimage178, 57–68, [PubMed: 29758339]

Yeh FC, Tseng WYI, 2011. NTU-90: a high angular resolution brain atlas constructed by q-space diffeomorphic reconstruction. Neuroimage58 (1), 91–99, [PubMed: 21704171]

Yeh FC, Verstynen TD, Wang Y, Fernández-Miranda JC, Tseng WYI, 2013. Deterministic diffusion fiber tracking improved by quantitative anisotropy. PLoS ONE8 (11), e80713. [PubMed: 24348913]

Yeo BTT, Krienen FM, Sepulcre J, Sabuncu MR, Lashkari D, Hollinshead M, Roffman JL, et al., 2011. The organization of the human cerebral cortex estimated by intrinsic functional connectivity. J. Neurophysiol106 (3), 1125–1165, [PubMed: 21653723]

Yeshurun Y, Carrasco M, 1998. Attention improves or impairs visual performance by enhancing spatial resolution. Nature396 (6706), 72–75. [PubMed: 9817201]

Yoo SA, Chong SC, 2012. Eccentricity biases of object categories are evident in visual working memory. Vis. cogn20 (3), 233–243.

Zalesky A, Fornito A, Cocchi L, Gollo LL, Breakspear M, 2014. Time-resolved resting-state brain networks. Proc. Natl. Acad. Sci. U.S.A111 (28), 10341–10346. [PubMed: 24982140]

Zanto TP, Gazzaley A, 2013. Fronto-parietal network: flexible hub of cognitive control. Trends Cogn. Sci17 (12), 602–603 (Regul. Ed.). [PubMed: 24129332]

Zhaoping L, 2017. Feedback from higher to lower visual areas for visual recognition may be weaker in the periphery: glimpses from the perception of brief dichoptic stimuli. Vis. Res136, 32–49. [PubMed: 28545983]
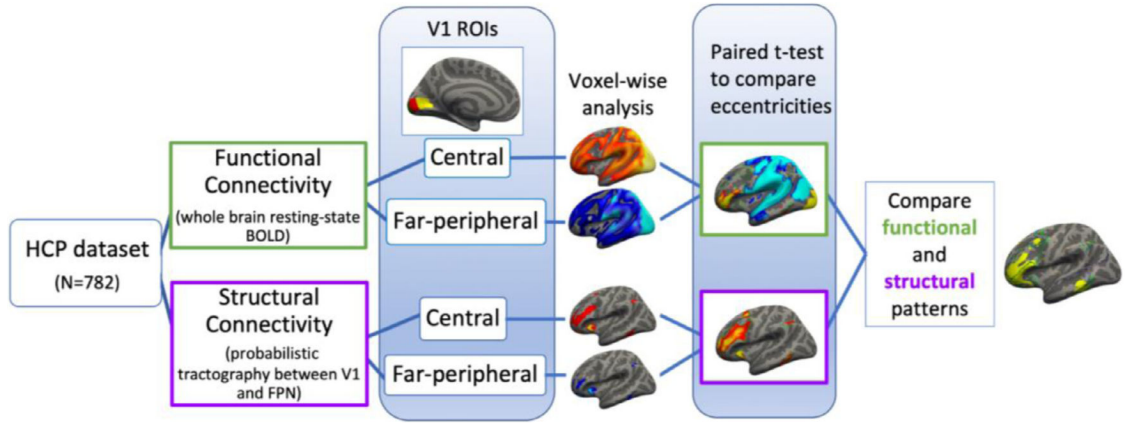
Fig. 1. Graphical representation of methods.
The figure illustrates from left to right: data used for the two main analyses, the analysis stream, and representations of the results. The top branch shows the analyses for functional connectivity and the bottom branch shows the analysis for structural connectivity. Voxel-wise connectivity to both the central and far-peripheral ROIs were calculated for both modalities. Then patterns of connectivity to central V1 and far-peripheral V1 were compared by paired *t*-test. The patterns from the comparison between central and far-peripheral V1 in both structural and functional modalities were overlaid and compared.
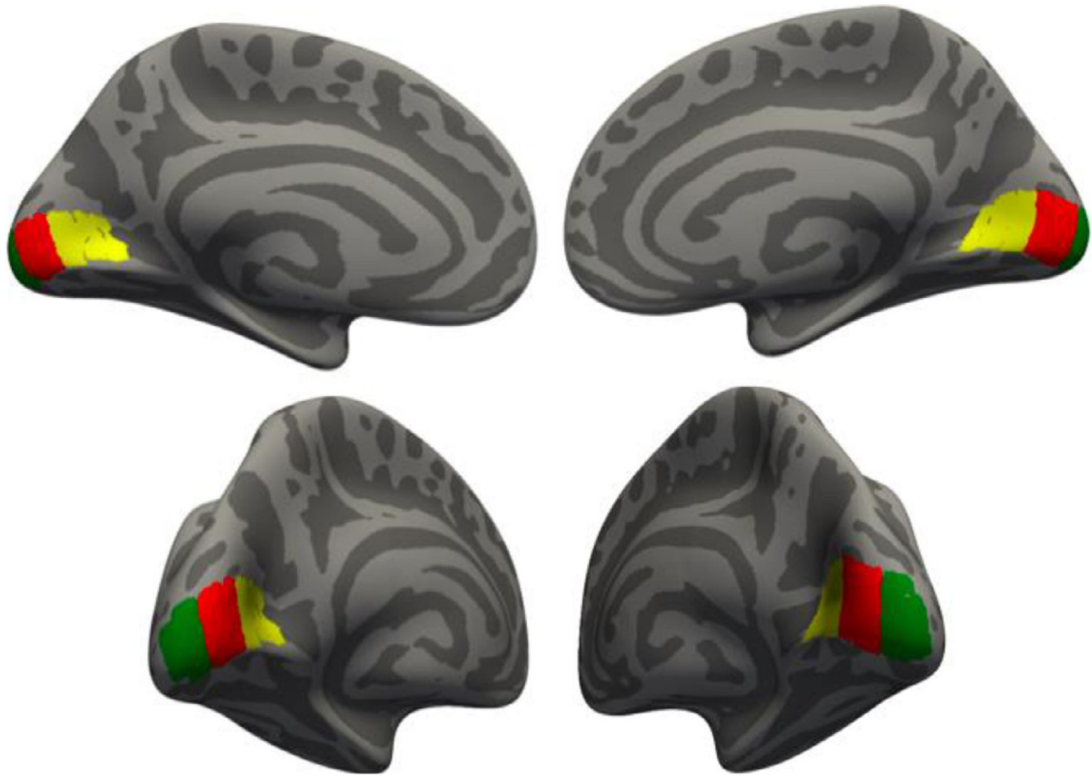
Fig. 2. V1 Eccentricity segments.
The Far-peripheral representing section of V1 is shown in yellow, the mid-peripheral representing section of V1 is shown in red, and the central representing section of V1 in green. These regions of V1 were used as seed regions in functional connectivity analyses. Central and far-peripheral ROIs were used as target regions for tractography analyses. We sometimes use shorthands like "central V1 " to refer to these centrally representing regions for brevity.
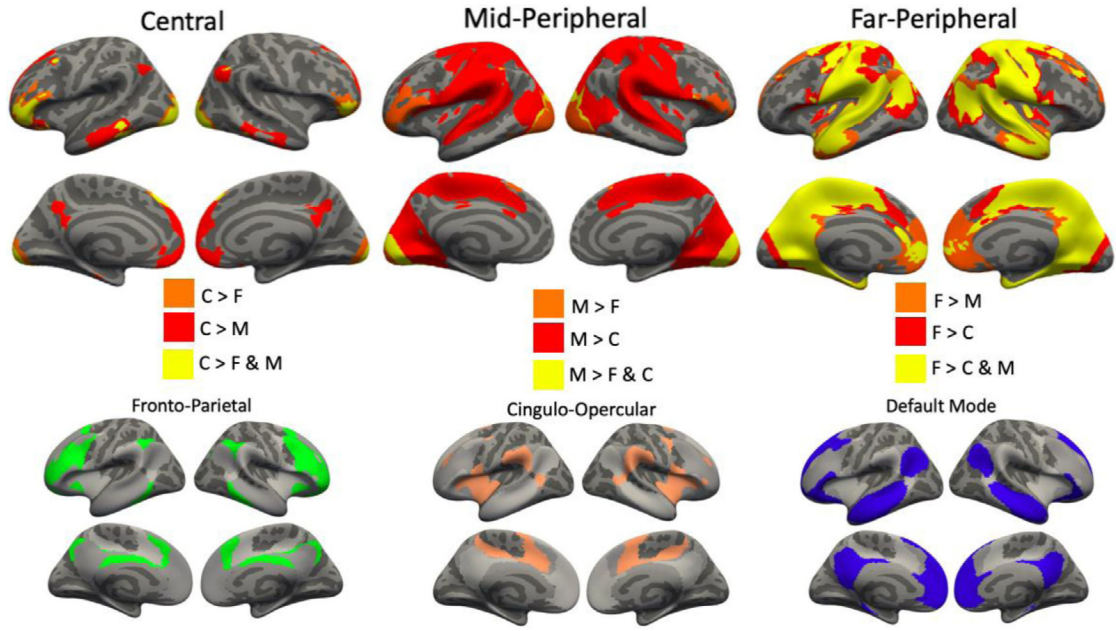
Fig. 3. Comparisons of functional connectivity between V1 eccentricity segments and homology to known resting-state networks.

Top Row: Differences in Functional Connectivity, depending on eccentricity. The far left panel highlights vertices with significantly stronger connections to central V1 than other portions of V1. Yellow vertices showed stronger connectivity to central V1 than to both far-peripheral and mid-peripheral regions (*C>F*&M). Red indicates stronger connectivity to central than mid-peripheral regions (*C>M*), and orange indicates stronger connectivity to central than far-peripheral regions (*C>F*). The middle and right panels show similar images highlighting vertices with significantly stronger connections to mid-peripheral and far-peripheral regions. For the middle panel, yellow is where mid-peripheral is greater than both central and far-peripheral (*M>F*&C), red is where mid-peripheral is greater than central (*M>C*), and orange is where mid-peripheral is greater than far-peripheral (*M>F*). For the panel on the right, yellow is where far-peripheral is greater than central and mid-peripheral(*F>C*&M), red is where far-peripheral is greater than central(*F>C*), and orange is where far-peripheral is greater than mid-peripheral(*F>M*). *Bottom Row:* Functional Networks for comparison to the top-row. Previously documented FPN, CON, and DMN (from Yeo et al., 2011). The FPN is shown in green, the CON is shown in tan, and the DMN is shown in blue. The gray regions in each image indicate the relative location of the other two networks for comparison. Note homologies between the FPN and the regions preferentially connected to Central V1 top row left panel.
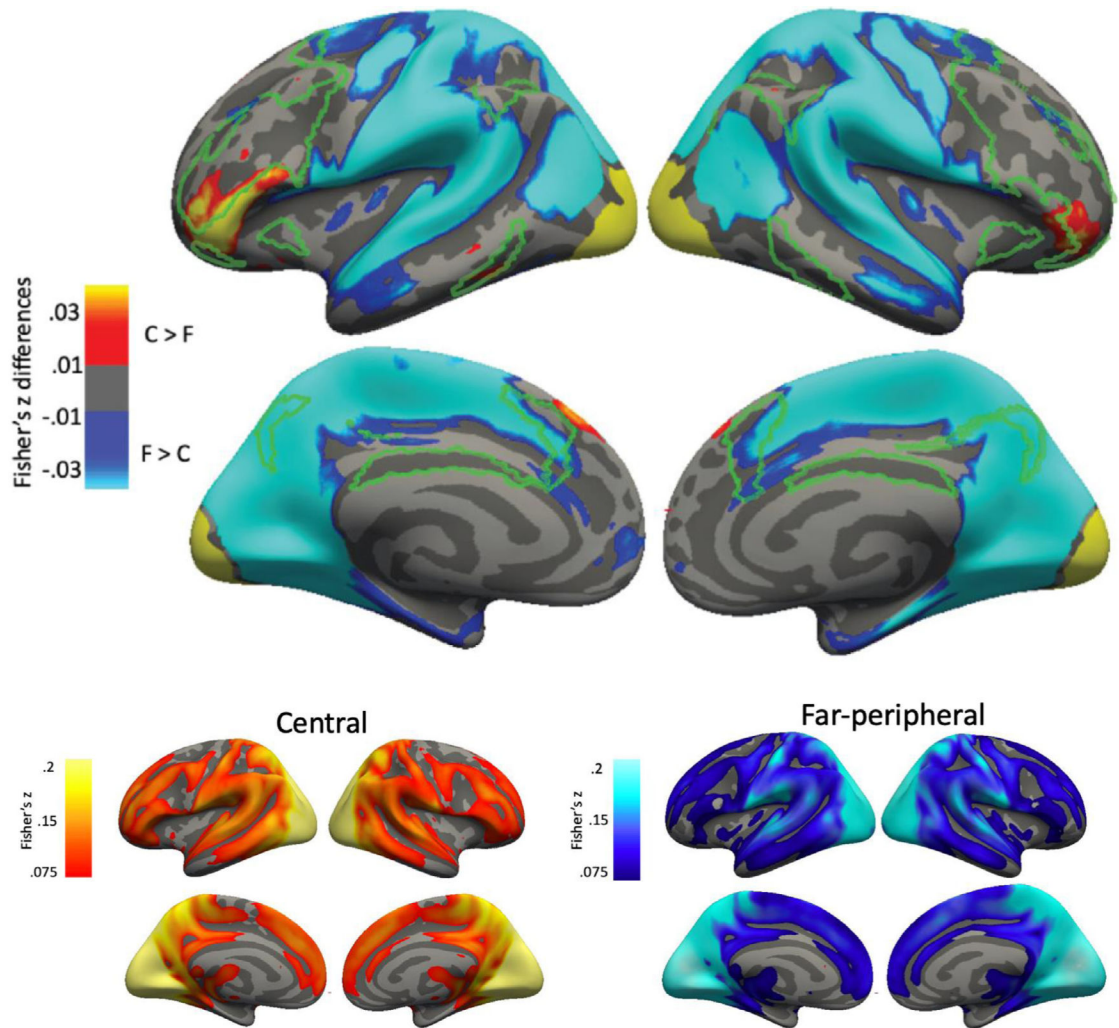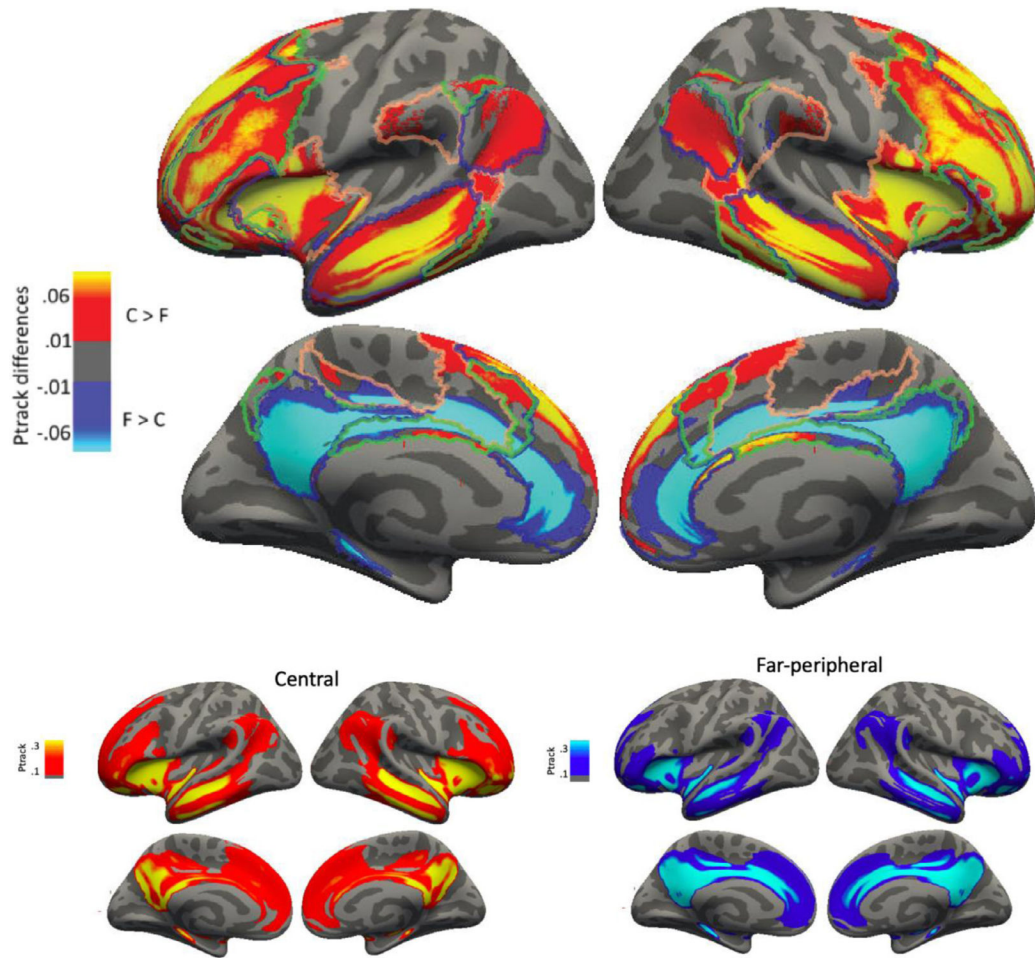
Fig. 4. Group average and statistical maps of comparisons of functional connectivity between V1 central and far-peripheral segments.

Top: Group average central minus far-peripheral differences in functional connections with the FPN. Group average data was thresholded for significance ($p < .001$) and effect size (connectivity differences > 0.01). The FPN is outlined in green. *Bottom:* Group average for central and peripheral functional connectivity. The top image is a subtraction between the data from the bottom two images.

Fig. 5. Group average and statistical maps of comparisons of structural connectivity between V1 eccentricity central and far-peripheral segments.
Top: Central (hot) minus Far-peripheral (cool) V1 structural connection differences to vertices within the FPN, CON, and DMN. Group average *p*-track differences between central and far-peripheral V1 data were thresholded for significance (*p* < .001) and effect size (*p*-track differences > 0.01) and masked for the FPN (outlined in green), DMN (outlined in dark blue), and CON (outlined in beige). *Bottom:* Group average for central and peripheral structural connectivity. The top image is a subtraction between the data from the bottom two images.
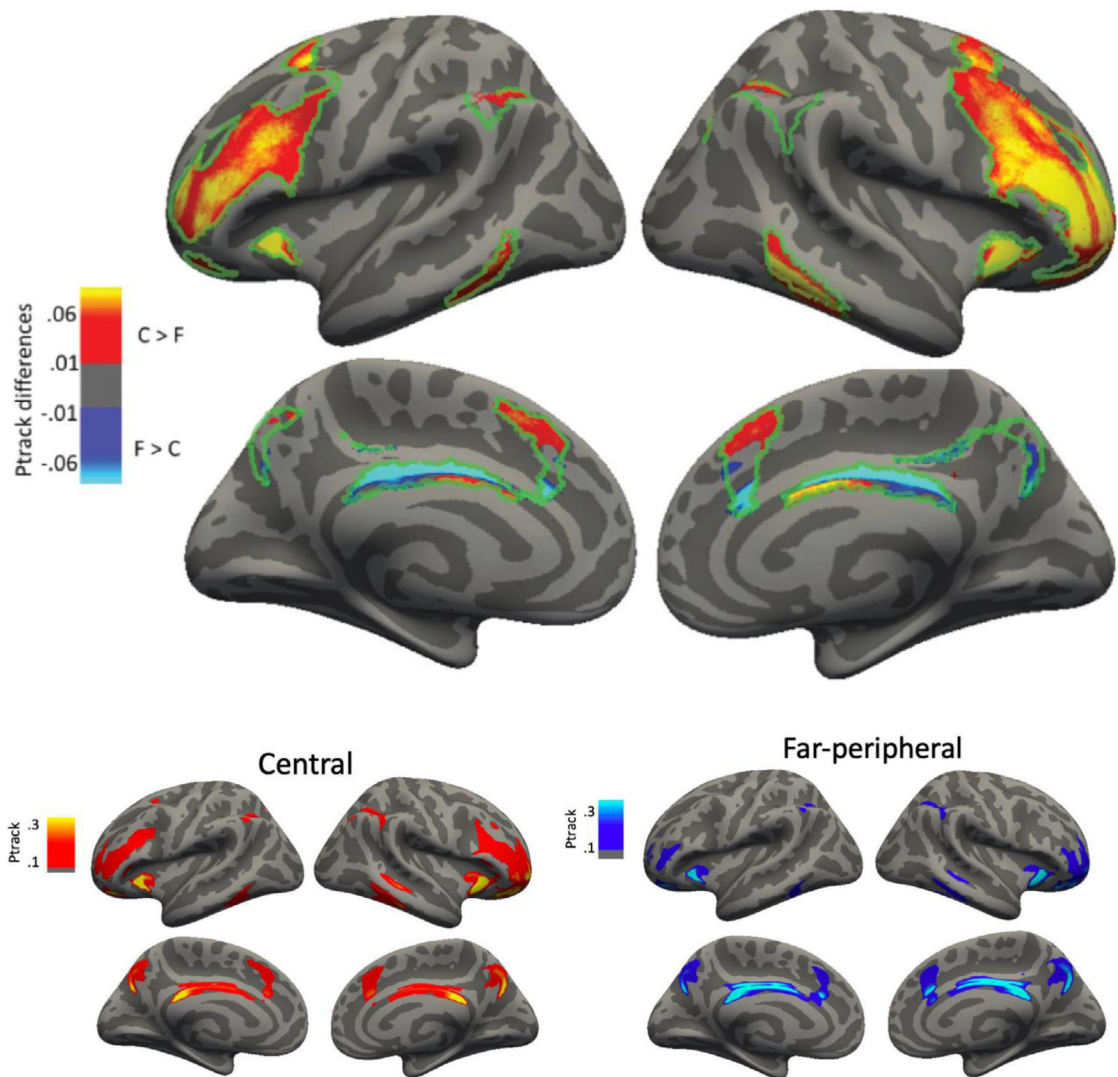
Fig. 6. Group average and statistical maps of comparisons of structural connectivity between V1 eccentricity central and far-peripheral segments.

Top: Central minus Far-peripheral V1 structural connection differences within the FPN. Group average p-track differences between central and far-peripheral V1 data were thresholded for significance ($p < .001$) and effect size (*p*-track differences > 0.01) and masked for the FPN (outlined in green). These data are the same as shown in Fig. 5, but are masked to show solely FPN to more clearly illustrate the effects present in that network. *Bottom:* Group averages for central and peripheral connectivity.
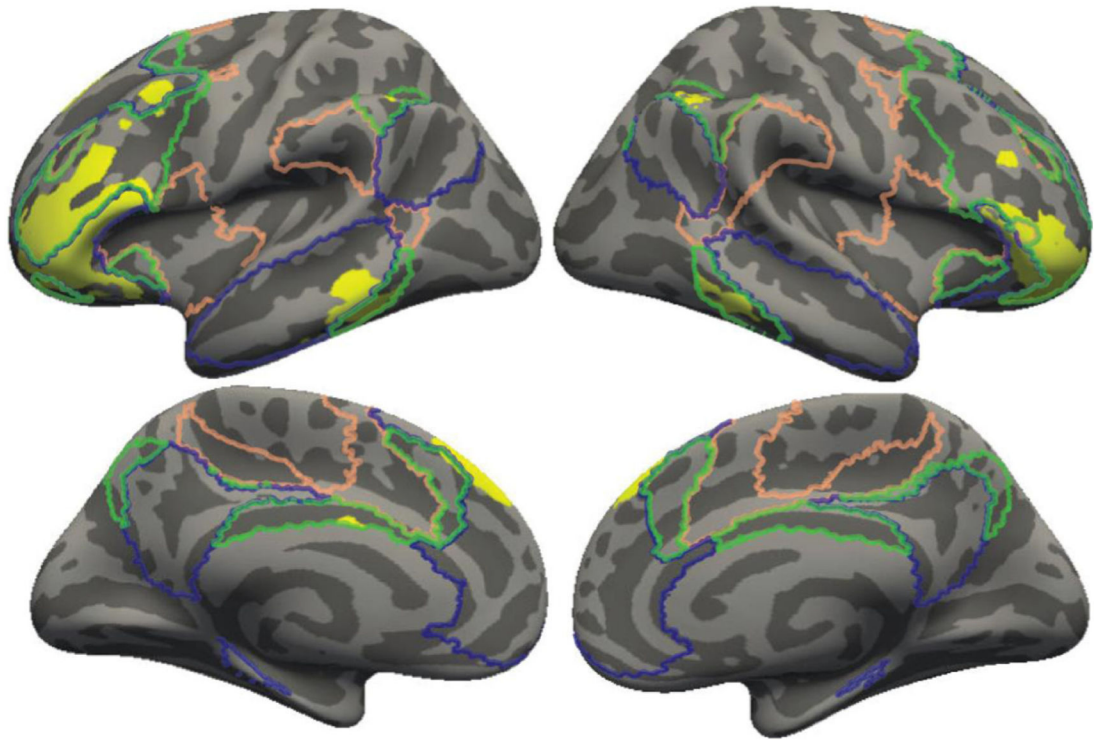
Fig. 7. Overlap of functional and structural connectivity patterns of central greater than far V1 eccentricity segments within resting-state networks (FPN (green outline), CON (beige outline), and DMN (dark blue outline)).

Yellow indicates vertices in which both structural p-track (Fig. 6) and functional connections (Fig. 4) were significantly greater to central V1 than far-peripheral V1 (both $p < .0001$).
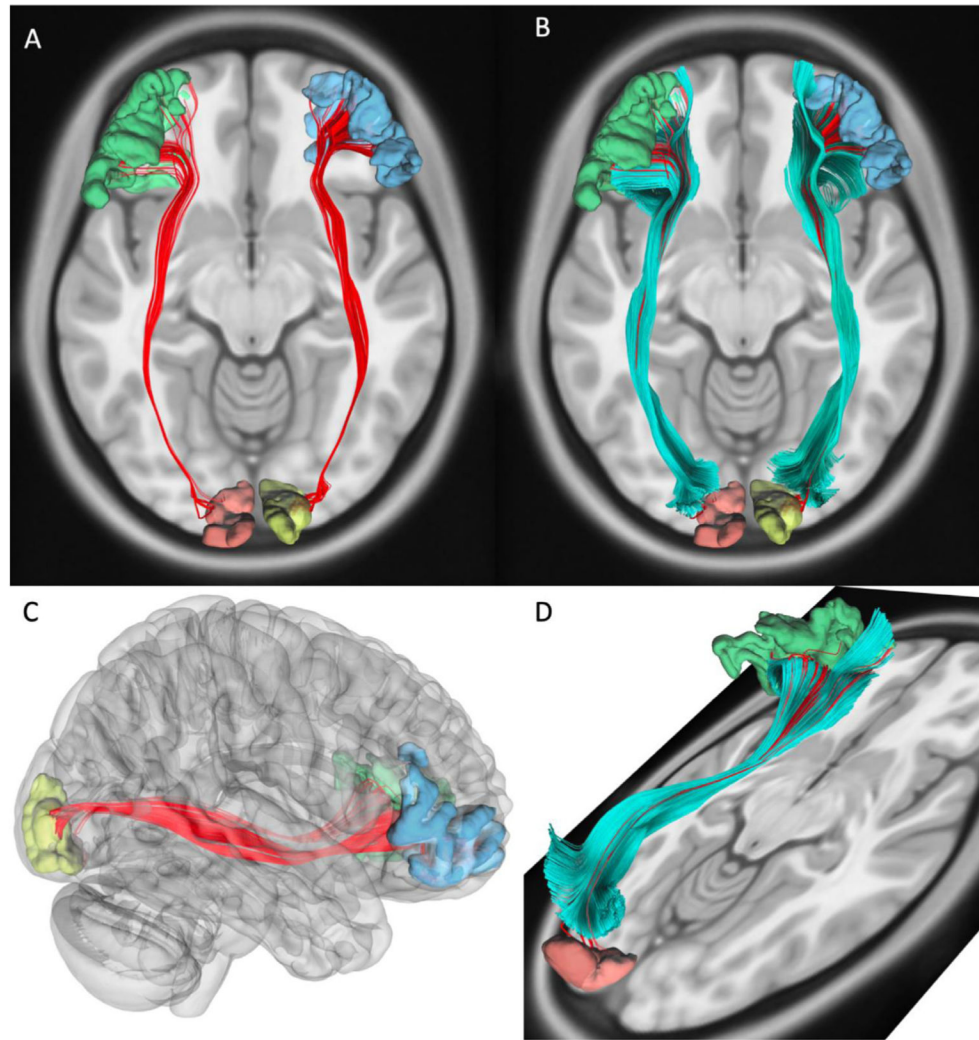
Fig. 8. Deterministic tractography between the frontal region identified in Fig. 7 and central V1.
Regions of interest: The green region is the left hemisphere frontal ROI, the blue region
is the right hemisphere frontal ROI, the orange region is left hemisphere central V1,
and the yellow region is right hemisphere central V1. A: Red tracks are results from
tractography between central V1 ROIs and frontal ROIs. B: Overlay of the IFOF (blue)
with the tractography results (red). C: Sagittal view of tractography results (red) with
the surface rendered. D: Horizontal slice (the same slice as parts A and B) with the left
hemisphere tractography results (red) and IFOF (blue) to view how the tractography results
are integrated into the IFOF.